Journal of Thermal Analysis Vol. 46 (1996) 1093-1111

Dedicated to Professor Bernhard Wunderlich on the occasion of his 65th birthday

ANALYSIS OF A SYMMETRIC NEOPOLYOL ESTER I. Measurement and calculation of heat capacity

M. Pyda[1], *Manika Varma-Nair*[2], *W. Chen*[1], *H. S. Aldrich*[2], *R. H. Schlosberg*[3] *and B. Wunderlich*[1]

[1]Department of Chemistry, The University of Tennessee, Knoxville, TN 37996- 1600; and Chemistry and Analytical Sciences Division, Oak Ridge National Laboratory, Oak Ridge, TN 37831-6197, USA
[2]Corporate Research, Exxon Research and Engineering Company, Linden, NJ 07036, USA
[3]Basic Chemicals and Intermediates Technology, Exxon Chemical Company, Clinton, NJ 08801, USA

Abstract

Quantitative thermal analysis was carried out for tetra[methyleneoxycarbonyl(2,4,4-trimethyl)pentyl]methane. The ester has a glass transition temperature of 219 K and a melting temperature of 304 K. The heat of fusion is 51.3 kJ mol^{-1}, and the increase in heat capacity at the glass transition is 250 J K^{-1} mol^{-1}. The measured and calculated heat capacities of the solid and liquid states from 130 to 420 K are reported and a discussion of the glass and melting transitions is presented. The computation of the heat capacity made use of the Advanced Thermal Analysis System, ATHAS, using an approximate group-vibration spectrum and a Tarasov treatment of the skeletal vibrations. The experimental and calculated heat capacities of the solid ester were compared over the whole temperature range to detect changes in order and the presence of large-amplitude motion. An addition scheme for heat capacities of this and related esters was developed and used for the extrapolation of the heat capacity of the liquid state for this ester. The liquid heat capacity for the title ester is well represented by $691.1 + 1.668\,T$ [J K^{-1} mol^{-1}]. A deficit in the entropy and enthalpy of fusion was observed relative to values estimated from empirical addition schemes, but no gradual disordering was noted outside the transition region. The final interpretation of this deficit of conformational entropy needs structure and mobility analysis by solid state ^{13}C NMR and X-ray diffraction. These analyses are reported in part II of this investigation.

Keywords: conformational disorder, crystal, DSC, glass, glass transition, heat capacity, melting transition, tetra[methyleneoxycarbonyl (2,4,4-trimethyl) pentyl] methane

Introduction

In this paper we present a characterization of the thermal properties of the symmetric pentaerythritol (or tetramethylol methane) ester: tetra[methylene-

0368–4466/96/ $ 5.00

John Wiley & Sons, Limited
Chichester

oxycarbonyl(2,4,4-trimethyl)pentyl]methane, abbreviated in this paper as MOCPM. Its chemical structure is ($C_{41}O_8H_{76}$, MW =697 Da):

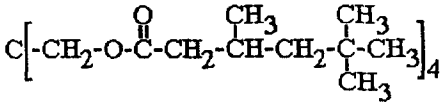

The discussion of the data will make use of the approach developed in the ATHAS Laboratory. Related compounds that were similarly analyzed are several polyesters [1, 2], as well as symmetric small molecules such as the long-chain tetraalkylammonium halides (TAAX [3, 4], and the liquid crystalline N,N'-*bis*(4-*n*-octyloxybenzal)-1,4-phenylenediamine (OOBPD) [5].

One of the problems in the discussion of heat capacity of solids and liquids concerns the deviation of the heat capacity from a baseline defined by the contribution from vibrational motion only. The determination of this baseline is fundamental to the study of glass and melting transitions as well as detection of conformational disordering.

It is well known that besides the three conventional states of matter: glass, crystal and melt, one can distinguish six mesophases as reviewed in Fig. 1. For example, a conformationally disordered crystal (condis crystal) has some or complete conformational disorder and mobility. A conformationally disordered

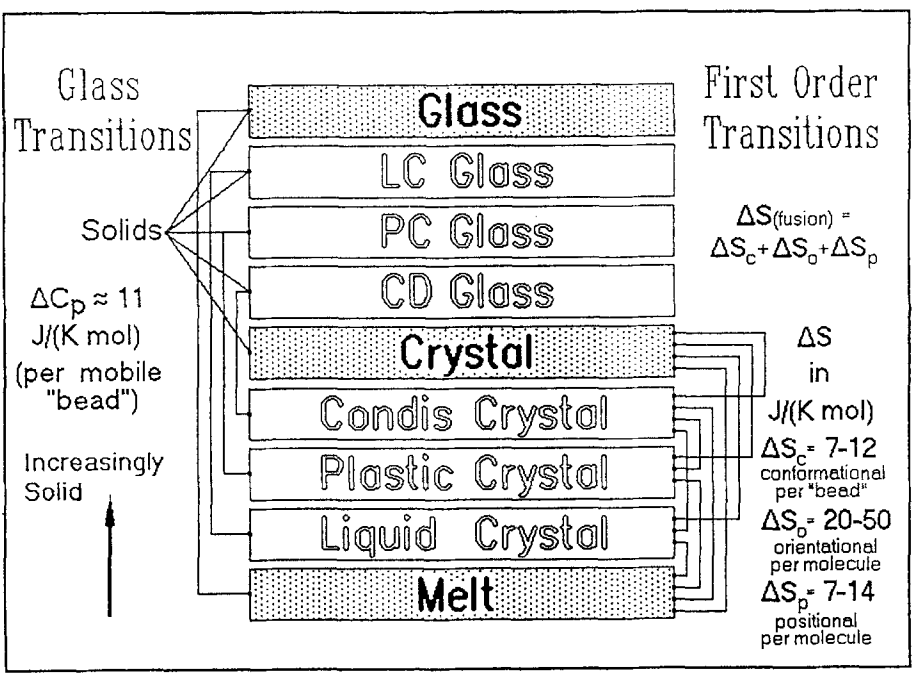

Fig. 1 Schematic of the various possible phases and mesophases and their transition entropies and changes of the heat capacity at the glass transition

glass (CD glass) has the same conformational disorder as the condis crystal, but its large-amplitude conformational motion, based on internal rotation, is frozen. In recent years, these mesophases have become easily recognizable by thermal analysis, using the empirical heat capacity and entropy contributions listed in Fig. 1 [6]. Going from a crystal to a liquid, the disordering can be estimated from its entropy of fusion:

$$\Delta S_{(\text{fusion})} = n\Delta S_c + \Delta S_o + \Delta S_p \quad (1)$$

where n is the number of rotatable bonds and $\Delta S_{(\text{fusion})} = \Delta H_f / T_f$ is the overall entropy of fusion of the compound (*i.e.* the transition entropy from the rigid, low-temperature crystal in one or several steps to the melt). Empirical rules of entropy changes at the transition from a crystal to the melt show, as summarized in Fig. 1, that the change in positional entropy, ΔS_p, is about 7–14 J K^{-1} mol^{-1}, and in orientational entropy, ΔS_o, about 20–50 J K^{-1} mol^{-1}. Both of these entropies refer to the molecule as a whole. The conformational entropy contribution, ΔS_c, of about 7–12 J K^{-1} mol^{-1} is, in contrast, to be counted per bond that changes its mobility (or "bead"), so that a single molecule may have more than one conformational contribution ($n\Delta S_c$). The total number of disordered bonds in the isotropic melt, n, can be estimated from the entropy of fusion *via* Eq. (1). On first inspection MOCPM may have, for example, as many as 4×7 bonds that can change their mobilty when going from the rigid crystal to the melt. The additional 16–CH_3-groups are known to become mobile at much lower temperatures and may rotate even within the "rigid" crystal. If, indeed, 28 bonds would become mobile on fusion, the entropy change should be about 310 J K^{-1} mol^{-1} (for more details, see below). Similarly, at the glass transition the heat capacity should increase by as much as 320 J K^{-1} mol^{-1} as each flexible bond (or "bead") contributes about 11.3 J K^{-1} mol^{-1} to the heat capacity.

Thermal analysis of different macromolecules and small molecules has led to the discovery of occasional deficits in the measured total entropy of fusion relative to the entropy estimated in the just outlined method. A few reasons for such deficits turned out to be:

- incomplete crystallization (this leads to partially crystalline samples, as is often seen in polymers),
- disorder gained outside the transition region (with an increase in heat capacity),
- disorder never lost during ordering on cooling (i. e. in the crystal certain parts of each molecule remain disordered, causing a condis crystal or a CD glass–the latter in case the conformational motion is frozen),
- some bonds of the molecule remain rigid, even in the isotropic melt.

The jump in heat capacity at T_g for a completely amorphous samples can be obtained experimentally for a quenched sample. The total mobility in the melt

can thus be estimated independently from both, the first-order disordering and fusion and the glass transition. Any possible deficit of entropy due to a gain in entropy outside of the transition region can then be assessed by comparing the heat capacity of the sample with the computed heat capacity due to vibrations from the ATHAS method [7].

Although thermal analysis can give an analysis of order and motion of a molecule as a function of temperature, details of the particular bonds and atoms involved, and sometimes also distinctions between transitions that cause the similar entropy changes, must be further analyzed by techniques such as solid state NMR, neutron scattering, and X-ray diffraction.

In this paper the transitions and heat capacities of MOCPM are reported and interpreted. Furthermore, an addition scheme is presented that permits prediction of the thermal properties of related compounds that have not been measured or even synthesized. A solid state ^{13}C NMR study of MOCPM and some X-ray data that support the thermal analysis results are to be reported separately [8].

Experimental

Sample

The sample of MOCPM is an Exxon Chemical Co. product of high purity and was analyzed as obtained. Typically such esters are prepared by reacting the polyol with an excess of monocarboxylic acid with or without added catalyst. Example catalysts are titanium tetraisopropoxide, zinc octoate, sulfuric acid, and p-toluenesulfonic acid. Temperature and pressure are chosen between 410 and 520 K and 4 and 100 kPa, respectively. If needed, remaining acidity can be neutralized. The ester is finished by treatment with alumina, activated carbon or clay and filtered. No impurities could be detected by NMR.

For storage, the sample was hermetically sealed and kept at room temperature. Because of the low melting temperature this is an annealing condition, i.e. as delivered, the sample was crystalline and was then measured with and without thermal pretreatment. To obtain the glassy phase, the sample was heated within the calorimeter to 333 K, then cooled at 15–20 K min^{-1} to 130 K, or quenched outside the calorimeter at about 400 K min^{-1}, using liquid nitrogen. The analysis of the quenched sample was more difficult because of condensation of water vapor on the sample pan. Since both methods gave indistinguishable thermal histories, most experiments were done using quick cooling inside the calorimeter.

Instrumentation and experiments

For measurement of the heats of transition and heat capacities of MOCPM, a commercial Thermal Analysis 2100 system from TA Instruments Inc. with a

912 Dual Sample DSC was used. Two different heads of the DSC were tested to obtain the best symmetry between sample and reference.

A single-run heat capacity technique was used. An empty pan, a sapphire reference, and the sample were placed on the three measuring positions. The details of this method for measurement of heat capacity were reported earlier [9–13]. All three aluminum pans were matched in weight to ±0.01 mg. The low-temperature measurements were performed with the standard liquid nitrogen cooling accessory [11, 12]. All heat capacities were measured with a heating rate of 10 K min^{-1}. Heat capacities were calibrated at each temperature with standard sapphire (Al_2O_3). The temperature calibration was carried out at the transitions of cyclohexane, 1-chlorobutane, hexane, naphthalene, indium, tin, and KNO_3. The samples with weights of 3–30 mg were enclosed in autosampler-type, sealed aluminum pans. No nitrogen gas was purged through the DSC cell during the low-temperature measurements. No significant weight loss was observed after several repeat measurements. The fluctuation of the initial isotherm was ±0.25 mW and the baseline changed by ±0.5 mW during heating (at 10 K min^{-1}).

The measured transitions and heat capacity data were averaged from two to four runs. The heat capacities of the MOCPM were determined in different temperature ranges: 130–213 K, 183–273 K, and 253–423 K. The average and standard deviations for the experimental heat capacity were estimated from all acceptable runs. The standard software for data analysis and calculation of the heat capacity was published earlier [11]. It includes corrections for temperature lag, heating rate, asymmetry, and nonlinear temperature calibration. Both slow cooling and annealing from 10 min to 6 h between the glass and melting transition temperatures led to practically no crystallization. The as-received crystalline samples could be duplicated by annealing at room temperature for more than three days.

Calculation of the heat capacity of the solid

The ATHAS method for the calculation of the heat capacity of solid molecules from approximate vibrational spectra has been applied to the experimental heat capacities [14–17]. In short, the experimental heat capacities at constant pressure C_p are converted to C_V according to the Nernst-Lindemann approximation [18]:

$$C_p - C_V = 3R_o A_o C_p \frac{T}{T_m} \tag{2}$$

where $A_o \approx 0.0039$ K mol J^{-1} and T_m, is the equilibrium melting temperature. The experimental C_V is then separated into the part that arises from group vi-

brations and that from skeletal vibrations. The latter is fitted to the Tarasov function to obtain two characteristic temperatures: Θ_1 and Θ_3. The first theta-temperature signifies the upper frequency limit of the intramolecular vibrations of a chain molecule, the second, the upper frequency limit of the intermolecular vibrations. Once the group-vibration contributions and the Tarasov function are known, one can calculate C_V(total) due to the approximate vibrational spectrum at any temperature. Because our experimental data of heat capacity started at 130 K, the fitted Θ_1 had to be coupled with a guess of Θ_3 for the low-frequency, intermolecular modes. At temperatures above Θ_3 each mole of these intramolecular modes contributes R, the gas constant, to the heat capacity.

In MOCPM there are a total of 125 atoms that lead to 375 modes of vibration. Of these one can extract a total of 268 group vibrations by comparison with prior analyzed molecules in the ATHAS data bank. The remaining 107 vibrations are assigned as skeletal vibrations. The skeletal vibrations consist of six modes related to the three translational and three rotational modes of the isolated molecule as a whole, and 101 modes resulting from the molecular skeleton. Table 1 displays more details about these vibrations. One can understand the approximate vibrational spectrum of MOCPM by referring to the neopentane skeleton [C(–C)$_4$] from which it is generated by insertion of four CH_2–O–CO–CH_2–C(CH_3)H–CH_2 chains at the bonds (–) and substitution of 12 methyl groups at the three free valences of the four (–C) atoms. A –CH_3-group with four atoms has 12 vibrational frequencies of which nine can be assigned as group vibrations by comparison with polypropylene (PP [19]), as listed in Table 2. The remaining three vibrations are assigned to the skeletal vibrations (approximately designated as one rotation and two bendings about the C–CH_3-bonds). Next follow the four C–C-bonds from the center of the molecule (five atoms =15 vibrational modes). The four C–C-stretching vibrations are assumed to be similar to those in a typical polymer chain, and listed also in Table 2. The remaining 11 modes are eight bending modes (which include the three rotations of the molecule as a whole) and three translational modes for the molecule. These 11 modes are added to the skeletal vibrations, raising the tally

Table 1 Number of groups and vibrations in MOCPM

Group	Number of groups and atoms in the molecule	Number of groups vibrations	Number of skeletal vibrations
–CH_3	$4 \times 3 = 12$	$(12 \times 9) = 108$	$(12 \times 3) = 36$
C(–C)$_4$	1	4	11
–CH_2–	$4 \times 2 = 8$	$8 \times 7 = 56$	$8 \times 2 = 16$
–CH_2–$CHCH_3$–	$4 \times 1 = 4$	$4 \times 20 = 80$	$4 \times 7 = 28$
–O–CO–	$4 \times 1 = 4$	$4 \times 5 = 20$	$4 \times 4 = 16$
Totals:		$N_g = 268$	$N_s = 107$

Table 2 Frequencies of the group vibration of MOCPM

Approximate vibrational mode	Frequency/K*	N_g /vibrators
$-CH_3$ (from PP [19])		
CH_3 asym. stretch	4262	1.0
CH_3 asym. stretch	4259	1.0
CH_3 sym. stretch	4147	1.0
C–CH_3 stretch	1568–1614	0.44
	1534–1614	0.56
CH_3 asym.bend	2107	1.0
CH_3 asym.bend	2101	1.0
CH_3 sym.bend	1987	0.25
	1973–1987	0.38
	1973	0.37
CH_3 rock	1453–1521	0.55
	1453	0.45
CH_3 rock	1361–1393	0.65
	1333–1361	0.21
	1336	0.14
C–C chain stretch (from PP [19])		
C–C stretch	1685	0.16
	1650–1685	0.84
$-CH_2-$ (from PE [19])		
CH_2 asym. stretch	4148	1.0
CH_2 sym. stretch	4098	1.0
CH_2 bend	2075	1.0
CH_2 wag	1698–1977	0.65
	1977	0.35
CH_2 twist	1874	0.52
	1690–1874	0.48
CH_2 rock	1494	0.04
	1038–1494	0.59
	1079	0.37
$-CH_2-CHCH_3$ (from PP [19])		
$-CH_3$ same as above		9.0
C–C stretch same as above		2.0
CH_2 sym. stretch	4085	1.0
CH_2 asym. stretch	4213	1.0
CH_2 wag	1876	0.18
	1842–1876	0.43
	1846	0.39
CH_2 twist	1722–1791	0.33
	1695–1722	0.55
	1695	0.12
CH_2 rock	1222–1295	0.52
	1289	0.48
CH stretch	4181	1.0

Table 2 (continuous)

Approximate vibrational mode	Frequency/K*	N_g /vibrators
CH bend	1963–1973	0.42
	1966	0.58
CH bend	1944	0.64
	1916–1944	0.28
	1916	0.08
C–CH_3 stretch	1568–1614	0.44
	1534–1614	0.56
–O–CO– (from Polyesters [20])		
C=O stretch	2530	1.0
CO–O stretch	1250	1.0
O–C stretch	1385	0.22
	1632	0.11
	1385–1632	0.67
C=O in-plane bend	980	1.0
C=O out-of plane bend	840	1.0

* Note that the frequencies are given in Kelvin (1.0 cm^{-1} ≐ 1.4388 K)

to 112 group vibrations and 47 skeletal vibrations. The remaining four linear chains that must be inserted to produce the MOCPM molecule consist each of two methylenes, as in polyethylene (PE [19]), one propylene, as in polypropylene [19], and one oxycarbonyl group, as in an aliphatic polyesters [20]. The totals of the number of vibrations are listed in Table 1, with the frequencies being shown in Table 2.

Results

Figures 2 and 3 show examples of the glass transition and fusion of the largely amorphous and largely crystalline MOCPM. The transition parameters are listed in Table 3. For the crystals one observes, depending on the thermal history, a more or less pronounced double melting transition. The main melting

Table 3 Examples of parameters of transition for semicrystalline MOCPM[a]

Parameter	Crystalline sample	Amorphous sample
T_f / K	275–300	–
	304	299[b]
ΔH_f / kJ mol^{-1}	47.1 (45)[c]	0.6
T_g / K	220	222(219)[c]
ΔC_p / J $K^{-1}mol^{-1}$	35.2	244(250)[c]

[a] For final data see text.
[b] The small amount of fusion may result from some cold crystallization during heating.
[c] Values in parentheses from the same traces, but after establishment of a C_p baseline.

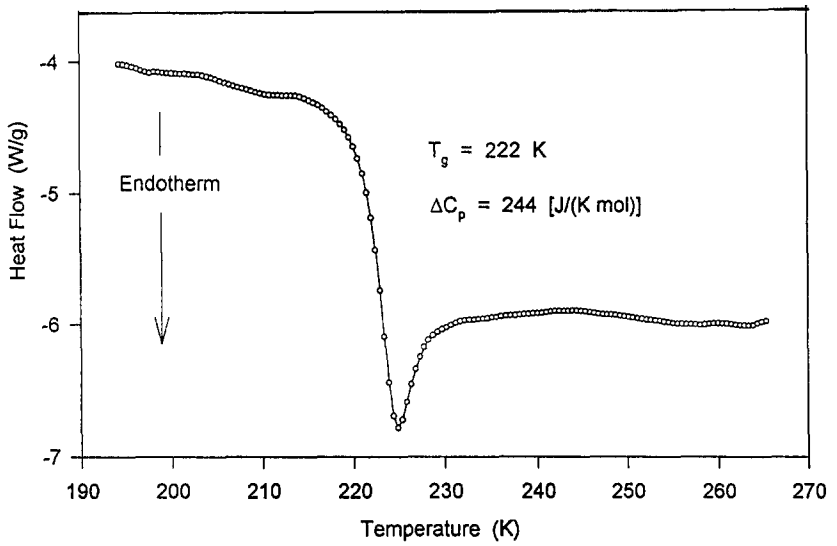

Fig. 2 Experimental DSC trace of quenched MOCPM in the glass transition region

peak is at T_f=304 K with a smaller, broad endotherm in the temperature range 275–300 K (Fig. 3). For less well crystallized samples than shown in Fig. 3, the low temperature fusion peak may be larger and sharper. The heat of fusion for the overall melting of a well crystallized sample is 47.1 kJ mol^{-1}. Using the

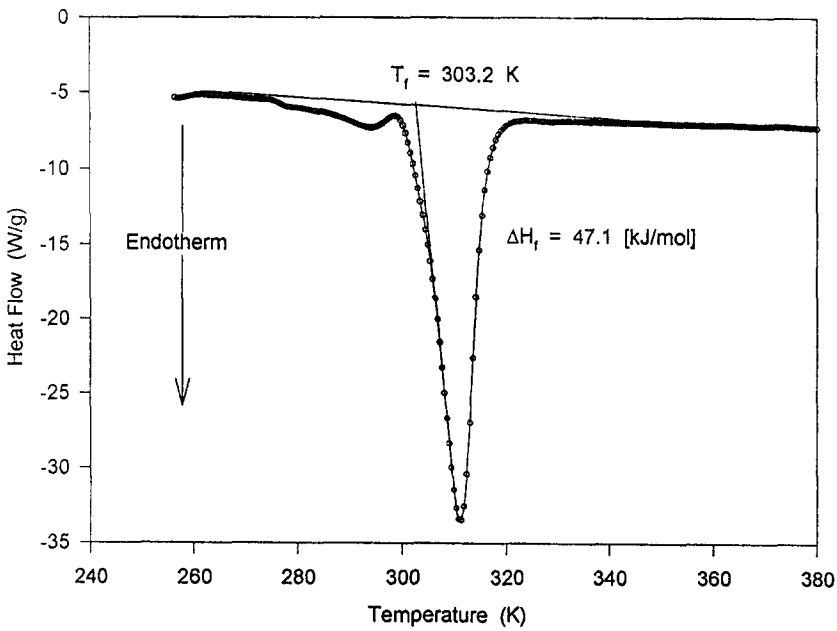

Fig. 3 Experimental DSC trace of MOCPM in the melting range

computed heat capacity as a base line, the peak area decreases slightly, to give a ΔH_f of 45 kJ mol^{-1}. The crystalline samples in Table 3 show a small glass transition at about the same T_g as the fully amorphous samples (see also Fig. 5, below). Data for additional samples are reported in Table 4. This suggests that perhaps none of the samples are fully crystalline. Extrapolation of the data in Table 4 to zero change in ΔC_p at T_g leads to 51.3 kJ mol^{-1} for the heat of fusion and a possible crystallinity of the best crystallized samples of about 88%.

Table 4 Change of the heat capacity at the glass transition ΔC_p as a function of ΔH_f

Heat of fusion ΔH_f /kJ mol^{-1}	Change of C_p at T_g ΔC_p /J K^{-1} mol^{-1}
48.6	34
47.1	35.2
46.2	40.0
45.3	49.5
0.6	244

The thermal properties of the amorphous state of MOCPM were measured on quenched samples, as detailed in the sample description. The glass transition was observed at 219 K with an endothermic hysteresis peak, and a change in heat capacity of about 250 J K^{-1} mol^{-1} (Table 3 and Fig. 4). Using the suggestion of Fig. 1, about 22 mobile units per molecule (250/11.3), or about 5.5 mobile units per branch could be involved in the glass transition.

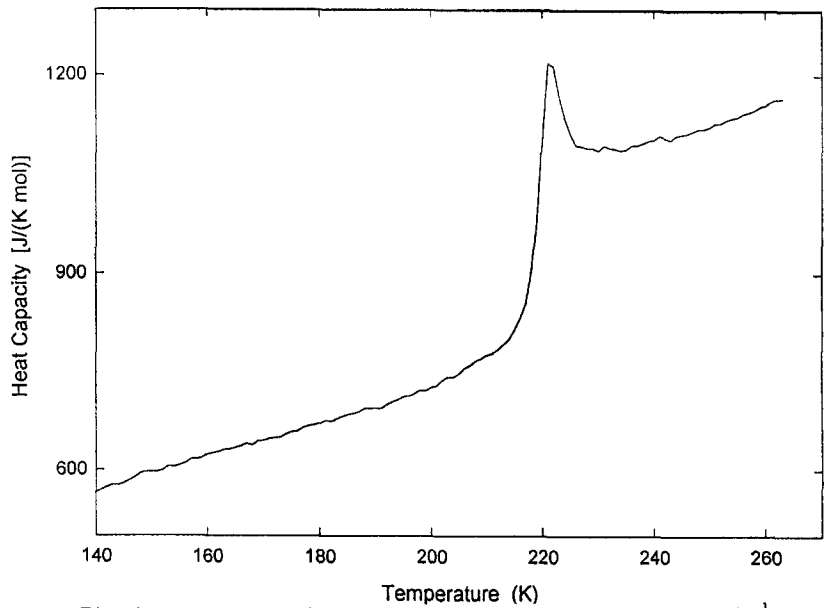

Fig. 4 Heat capacity of amorphous MOCPM measured at 10 K min^{-1}

Table 5 Measured and calculated heat capacities starting with crystalline MOCPM

Temperature/ K	Measured C_p / J K^{-1} mol^{-1}	Calculated[a] C_p / J K^{-1} mol^{-1}	Deviation/ %
130	522.49	510.41	–2.31
140	567.06	545.89	–3.73
150	593.15	580.44	–2.14
160	623.35	614.13	–1.48
170	647.86	647.36	–0.08
180	679.60	680.35	0.11
190	706.46	713.16	0.95
200	745.58	745.53	–0.01
210	776.41	778.15	0.22
219(T_g)		807.58	
220	849.12	810.85	–4.51
230	868.43	845.23	–2.67
240	898.55	878.06	–2.28
250	922.37	912.87	–1.03
260	945.70	947.84	0.23
270	982.78	983.17	0.04
273.15	1024.30	994.47	–2.91
280	1120.89	1020.66	–8.94
290	1335.38	1056.66	–
298.15	1855.71	1087.04	–
300	1973.82	1093.88	–
304(T_f)	3004.45	1095.70	–
310	4550.39	1131.75	–
320	1235.86	1169.62	–
	Melt		
320	1235.86	1224.86	–0.89
330	1240.17	1241.54	0.11
340	1257.33	1258.22	0.07
350	1284.66	1274.90	–0.76
360	1300.27	1291.58	–0.67
370	1321.47	1308.26	–1.00
380	1346.08	1324.94	–1.57
390	1361.49	1341.62	–1.46
400	1381.30	1358.60	–1.66
410	1400.90	1374.98	–1.85

[a] From 130 to 320 K data are calculated from approximate frequency spectra, from 320 to 410 K by equation (13A)

Results of the heat capacity measurements of the crystallized, glassy, and liquid MOCPM are presented from 130 to 410 K in Tables 5 and 6, and are plotted in Fig. 5. The experimental heat capacities for all solids were averaged below the glass transition temperature (from 130 to 210 K) and fitted to the approximate vibrational spectrum using the ATHAS Computation Scheme,

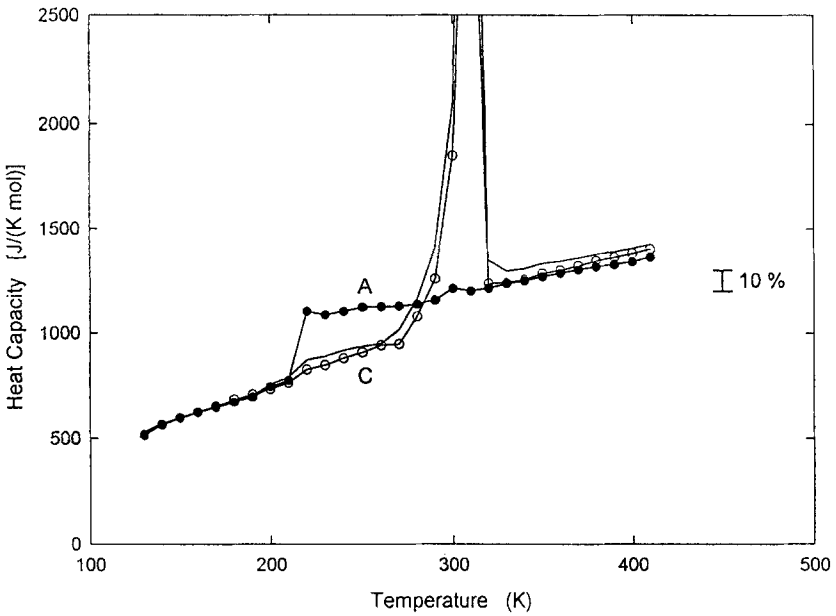

Fig. 5 Experimental heat capacity of two almost crystalline (*C*) and one amorphous (*A*) MOCPM, measured at 10 K min^{-1}

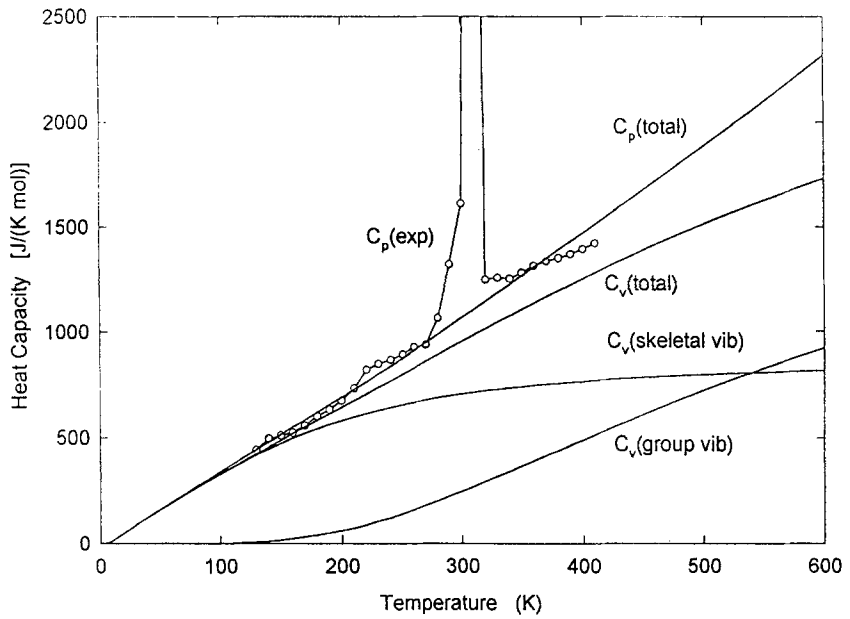

Fig. 6 Calculated and experimental heat capacity for MOCPM from the approximate vibrational spectrum of Table 2, $\Theta_1 = 750$ K, and $\Theta_3 = (100$ K) (estimated), using the ATHAS scheme

Table 6 Measured and calculated heat capacities starting with glassy MOCPM

Temperature/ K	Measured C_p / J K^{-1} mol^{-1}	Calculated* C_p / J K^{-1} mol^{-1}	Deviation/ %
	Solid		
130	513.81	510.41	-0.66
140	565.55	545.89	-3.48
150	597.41	580.44	-2.84
160	623.52	614.13	-1.51
170	644.46	647.36	0.45
180	671.11	680.35	1.38
190	694.48	713.16	2.69
200	745.64	745.53	0.06
210	774.69	778.15	0.45
219(T_g)	911.13	807.58	
	Liquid*		
219(T_g)	931.13	1056.40	
220	1103.84	1058.06	-4.15
230	1086.30	1074.74	-1.06
240	1103.08	1091.42	-1.06
250	1123.04	1108.10	-1.33
260	1125.89	1124.78	-0.10
270	1128.41	1141.46	1.16
273.15	1131.61	1146.71	1.34
280	1138.52	1158.14	1.72
290	1157.78	1174.82	1.47
298.15	1203.22	1188.41	-1.23
300	1213.54	1191.50	-1.82
310	1200.87	1208.18	0.60
320	1214.14	1224.86	0.88
330	1235.49	1241.54	0.49
340	1248.78	1258.22	0.76
350	1270.30	1274.90	0.36
360	1285.49	1391.58	0.47
370	1303.09	1308.26	0.40
380	1317.38	1324.94	0.57
390	1327.76	1341.62	1.04
400	1341.93	1358.30	1.22
410	1364.67	1374.98	0.76

* For the glass (up to 219 K, data are calculated from approximate frequency spectra as for the crystal (Table 5), the values for C_p of the liquid from 219 K on are derived from the Eq. (13A): $C_p = 691.1 + 1.668T$

described above. As was mentioned earlier, the vibrational spectrum used was approximated with 107 skeletal and 268 group vibrational modes as given in Tables 1 and 2. The best fit over the full temperature range was found for a values of $\Theta_1 = 750$ K. For an estimate of the lower heat capacities, Θ_3 was guessed to

be 100 K. For A_o, the approximate, universal value of 0.0039 K mol J^{-1} had to be used. The average error is –0.8% and the RMS error is ±1.6% (Tables 5 and 6). Figure 6 illustrates the various computed and experimental data.

The measurements of the heat capacity for the liquid state of MOCPM were made on the glassy sample above T_g (from 230 to 280 K) and on the highly crystalline samples, above the melting temperature (from 320 to 410 K). The averaged results were fitted to the following equation:

$$C_p = 692.6 + 1.668\ T \qquad (4)$$

which resulted in a regression error r^2 of 0.992, an average deviation of +0.06% and an RMS error of ±0.8%.

Discussion

Glass and melting transitions

The results on the heat of fusion and the melting temperature permit a calculation of the entropy of fusion, ΔS_f. For the extrapolated, 100% crystalline sample, this calculation leads to 51300/304 = 168.8 J K^{-1} mol^{-1}. Assuming that the MOCPM molecule has, as outlined in the Introduction, full mobility in the melt, one expects 28 flexible bonds to change conformations on fusion. This would give, according to Fig. 1, a conformational entropy of fusion of about 266 J K^{-1} mol^{-1}, in addition to the positional and orientational contributions of about 45 J K^{-1} mol^{-1}. There must thus either be some deficit to the entropy of fusion at the transition, or the molecule is sterically so hindered that only (169–45)/9.5 ≈ 13 bonds become mobile in the melt (about three per branch).

The glass transition in Fig. 2 looks quite normal, showing a small hysteresis peak. The ratio of melting transition to glass transition temperature is also as found for many similar molecules, about 1.4. The increase of the heat capacity at the glass transition suggests, as reported above, that there are about 22 "beads" that become mobile at the glass transition, *i.e.* the molecule can not be as rigid as the entropy of fusion would indicate if the assumption of a rigid molecule were true. The increase in heat capacity at the glass transition suggests that of the seven bonds in each branch of the molecule that may become mobile, approximately five do. This would leave a deficit in entropy of fusion of about two bonds per chain.

The deficit in the entropy of fusion corresponding to two bonds gaining conformational disorder on melting must be explained by the remaining two reasons listed in the Introduction: There may be a disordering outside the transition region, or the crystals are condis crystals or CD glasses. Both possibilities were observed in sterically complicated molecules [3–5]. The heat capacities discussed next, exclude the possibility of disordering outside of the

transition region since the crystalline samples follow the heat capacity calculated under the assumption of vibrations only. This leaves only the possibility of conformational disorder in the crystal. Furthermore, since there seems to be no second glass transition for the disorder in the crystal, the conformational disorder must be frozen as a CD glass (Fig. 1).

Heat capacities of solid MOCPM

The measured solid heat capacities agree well with the computed ones up to the glass transition region (210 K) or the melting region (270 K). This permits no significant disordering before the melting range (Figs 5 and 6 and Tables 5 and 6). Using the calculated heat capacity of the approximate vibrational spectrum as baseline, the heat fusion of Table 3 was corrected to 45 kJ mol^{-1}.

In order to discuss the relation between $\Theta_1=750$ K and the structure of MOCPM, one notes that a similar value of Θ_1 of 850 K was found for polyisobutylene (PIBUT) (fitted between 120 and 190 K) [20]. It may indicate that for MOCPM, as in PIBUT, the $-C(CH_3)_x$ groups dominate the intramolecular heat capacity contribution of the skeletal vibrations to the heat capacity at low temperature.

Heat capacities of MOCPM in the liquid state

Most experimental heat capacities of liquid macromolecules exhibit a linear temperature dependence [21–23]. One expects, similarly, that over a reasonable temperature range, the heat capacity of MOCPM is linear and Eq. (4), extracted from data between 230 and 410 K may be extrapolated to higher and lower temperatures.

Addition scheme for the liquid heat capacity for MOCPM and retated compounds

Using the empirical addition scheme in our ATHAS Laboratory for liquid heat capacities [21–22], C_p(liquid) was calculated for the temperature range of 210–410 K. The total heat capacities of the molecule was obtained from contributions of the various structural groups:

1. The methylene group [CH_2–] not connected to the [COO–] group:

$$C_p=17.92+0.0433\,T \tag{6}$$

2. The methylene group [CH_2–] connected with a [COO–] group:

$$C_p=13.7711+0.0471\,T \tag{7}$$

3. The oxycarbonyl group [O–CO–]:

$$C_p = 64.32 + 0.00244\ T \tag{8}$$

4. The isopropylidene group [$C(CH_3)_2$–]:

$$C_p = 18.79 + 0.2013\ T \tag{9}$$

5. The methylmethylene group [$CHCH_3$–]:

$$C_p = 25.05 + 0.108\ T \tag{10}$$

6. The methyl group [CH_3–]:

$$C_p = 30.41 + 0.01479\ T \tag{11}$$

To obtain a contribution of the heat capacity for the quaternary carbon group $C(-)_4$, an equation was derived from the experimental heat capacity of liquid 2,2-dimethylbutane (2,2-DMB) that is given by $C_p = 94.1 + 0.313\ T$ [24]. By subtracting contributions from the extra methylene and the methyl groups one obtains the following result:

7. The quaternary carbon atom $C(-)_4$:

$$C_p = -44.87 + 0.2093\ T \tag{12}$$

The contribution from the quaternary carbon group is negative only for $T < 214$ K.

Based on this addition scheme the liquid heat capacity of MOCPM can be expressed as:

$$C_p = 691.1 + 2.07\ T \text{ in } [\text{J K}^{-1} \text{ mol}^{-1})] \tag{13}$$

The comparison of the experimental data of heat capacity with results obtained from Eq. (13) shows an average deviation of about +10% and an RMS of 1.4% in the temperature range 230–410 K. It should be pointed out that differences in the experimental and addition scheme liquid heat capacities for materials with ester groups had been reported before for some aliphatic polyesters [1, 22]. It was shown that the ester group contributions to the total liquid heat capacity depends to some degree on the positioning of [O–CO–] and the number of [CH_2–] groups. Different contributions were derived for different esters. This suggests that the here used fit to a linear addition scheme needs correction to the experimental slope of Eq. (4). This correcting changes Eq. (13) to:

$$C_p = 691.1 + 1.668\ T \text{ in } [\text{J K}^{-1} \text{ mol}^{-1}] \tag{13A}$$

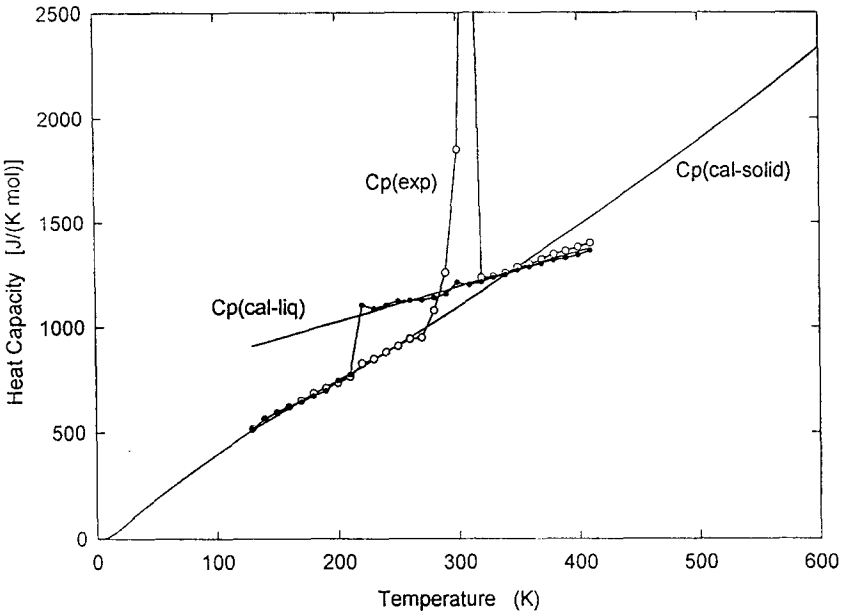

Fig. 7 Calculated heat capacity for liquid MOCPM from the addition scheme [Eq. (13A)], compared to the solid heat capacity calculated from the vibrational spectrum and the experimental data for an amorphous (•) and a crystalline sample (o)

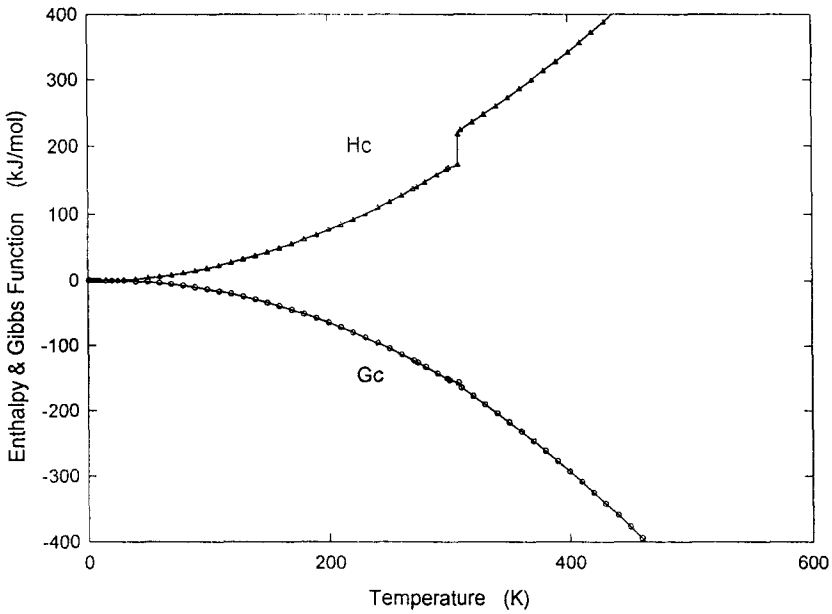

Fig. 8 Thermodynamic functions of MOCPM. (Note that the values of *G* decrease with temperature, those of *H* increase, and *TS* is the (positive) difference of the two curves shown)

This new equation agrees with the experiment to an average deviation of 0.3% and an RMS of ±0.96% in the temperature range from 230 to 410 K, or with an average deviation of –0.1% and an RMS of ±0.3% in the temperature range 320–410 K (Tables 5 and 6 for data). Figure 7 displays experimental and calculated heat capacities according to Eq. (13A).

The increase in heat capacity taken directly from the heat capacity corrected DSC traces was 250 J K^{-1} mol^{-1} and is taken as the measured quantity. The computed solid heat capacity coupled with the experimental, averaged liquid heat capacities [Eq. (4)] gives 250.3 J K^{-1} mol^{-1} and with the corrected addition scheme, 248.8 J K^{-1} mol^{-1}. These small deviations are within the experimental error limit of about 0.5% for ΔC_p and do not affect the discussion of the deficit of the entropy of fusion.

Thermodynamic functions

Thermodynamic functions: enthalpy, entropy and Gibbs free energy can be calculated easily from the heat capacity by integration of C_p and C_p/T and calculation of $H–TS$, respectively. Addition of information on heats of formation (from heats of combustion) can complete the thermodynamic characterization. Figure 8 shows the calculations for the crystalline sample.

Conclusions

1. A quantitative thermal analysis of MOCPM has been completed.

2. The ATHAS scheme of computation of solid and liquid heat capacities, derived originally for linear macromolecules [14–17], was applied to short-chain molecules. A comparison to similar analyses of normal paraffins [25], perfluoroparaffins [26], OOBPD [5], and TAAX [3, 4] suggests that about six atoms linked in a sequence is the lower limit to treat the molecule as a linear chain.

3. The heat capacity showed no gradual changes in conformational disorder outside the transition regions, a point of importance for the interpretation of the NMR and X-ray data [8].

4. Based on the discussion of the entropy of fusion and increase of ΔC_p at T_g it is likely that about two bonds per branch of the molecule remain rigid, even in the melt, and an average of two additional bonds per branch remain conformationally disordered on crystallization.

5. More structural evidence is given in Paper II [8]. It will be shown that the material is, indeed semicrystalline, but in addition, some of the branches of the crystallized molecules remain conformationally disordered. The disorder may be caused by the chiral centers in the branches.

* * *

The work of M. P. was supported by the Exxon Research and Engineering Company, New Jersey, under Contract #C07-C3185. Helpful discussions on instrumentation by Mr. A. Boller and Dr. Y. Jin are acknowledged.

The ATHAS group is supported by the Division of Materials Research, National Science Foundation, Polymers Program, Grant # DMR 90-00520 and the Division of Materials Sciences, Office of Basic Energy Sciences, U. S. Department of Energy, under Contract DE-AC05-84OR21400 with Lockheed Martin Energy Systems, Inc.

References

1 M. Varma-Nair, R. Pan and B. Wunderlich, J. Polymer Sci., Part B, Polymer Phys., 29 (1991) 1107.
2 J. Grebowicz, M. Varma-Nair and B. Wunderlich, Polym. Adv. Technol., 3 (1992) 51.
3 A. Xenopoulos, J. Cheng, M. Yasuniwa and B. Wunderlich, Mol. Cryst. Liq. Cryst., 214 (1992) 63.
4 A. Xenopoulos, J. Cheng and B. Wunderlich, Mol. Cryst. Liq. Cryst., 226 (1992) 87.
5 J. Cheng, Y. Jin, G. Liang, B. Wunderlich and H. G. Wiedemann, Mol. Cryst. Liq. Cryst., 213 (1992) 237.
6 B. Wunderlich, "Macromolecular Physics, Volume 3, Crystal Melting." Academic Press, New York, 1980; and B. Wunderlich, M. Möller, J. Grebowicz and H. Baur, "Conformational Motion and Disorder in Low and High Molecular Mass Crystals." Springer Verlag, Berlin, 1988, (Adv. Polymer Sci., Volume 87).
7 B. Wunderlich, Pure Applied Chem., 67 (1995) 1919.
8 W. Chen, M. Pyda, M. Varma-Nair, H. S. Aldrich and B. Wunderlich, J. Thermal Anal., 46 (1996) 1113.
9 B. Wunderlich, J. Thermal Anal., 32 (1987) 1949.
10 Y. Jin and B. Wunderlich, J. Thermal Anal., 36 (1990) 1519.
11 Y. Jin and B. Wunderlich, J. Thermal Anal., 38 (1992) 2257.
12 Y. Jin and B. Wunderlich, Proc. 21st NATAS Conf., Atlanta GA, Sept. 1992, p. 151–156.
13 Y. Jin and B. Wunderlich, Thermochim. Acta, 226 (1993) 155.
14 Yu. V. Cheban, S.-F. Lau and B. Wunderlich, Colloid Polymer Sci., 260 (1982) 9.
15 S.-F. Lau and B. Wunderlich, J. Thermal Anal., 28 (1983) 59.
16 R. Pan, M. Varma-Nair and B. Wunderlich, J. Thermal Anal., 36 (1990) 145.
17 J. Grebowicz and B. Wunderlich, J. Thermal Anal., 30 (1985) 229.
18 R. Pan, M. Varma-Nair and B. Wunderlich, J. Thermal Anal., 35 (1989) 955.
19 H. S. Bu, W. Aycock and B. Wunderlich, Polymer, 28 (1987) 1165.
20 S. Lim and B. Wunderlich, Polymer, 28 (1987) 777.
21 U. Gaur, M.-Y. Cao, R. Pan and B. Wunderlich, J. Thermal Anal., 31 (1986) 421.
22 R. Pan, M.-Y. Cao and B. Wunderlich, J. Thermal Anal., 31 (1986) 1319.
23 S. Z. D. Cheng, R. Pan, H. S. Bu, M.-Y. Cao and B. Wunderlich, Makromolekulare Chemie, 189 (1988) 1579.
24 D. R. Dousilu and H. M. Huffman, J. Am. Chem. Soc., 68 (1942) 1707.
25 Y. Jin and B. Wunderlich, J. Phys. Chem., 95 (1991) 9000.
26 Y. Jin, A. Boller, B. Wunderlich and B. V. Lebedev, Thermochim. Acta, 234 (1994) 103.